Polymer 50 (2009) 2503–2509

Contents lists available at ScienceDirect

Polymer

journal homepage: www.elsevier.com/locate/polymer

[NCO]/[OH] and acryl-polyol concentration dependence of the gelation process and the microstructure analysis of polyurethane resin by dynamic light scattering

Takuya Suzuki [a], Mitsuhiro Shibayama [a,*], Kazuhiro Hatano [b], Masahiko Ishii [b]

[a] Institute for Solid State Physics, The University of Tokyo, 5-1-5 Kashiwanoha, Kashiwa, Chiba 277-8581, Japan
[b] Paint & Finishing Design Dept., Vehicle Material Engineering Div., Toyota Motor Corporation, 1, Toyota-cho, Aichi 471-8572, Japan

ARTICLE INFO

Article history:
Received 5 October 2008
Received in revised form
13 March 2009
Accepted 22 March 2009
Available online 27 March 2009

Keywords:
Polyurethane resin
Dynamic light scattering
Gelation

ABSTRACT

The gelation process and the microstructure after the gelation of polyurethane resin consisting of acryl-polyol and polyisocyanate was investigated by dynamic light scattering (DLS) as a function of stoichiometric ratio, [NCO]/[OH], and the concentration of acryl-polyol, C_{polyol}. The following conclusions were obtained. First, the sol–gel transition was explained by the so-called site–bond percolation theory. Here polyol groups act as site-occupants, and isocyanate groups act as chemical cross-linkers. Second, the scattering inhomogeneities increased rather gradually around the gelation point, which are the characteristics of the gelation process not from monomeric but from oligomer units. Third, at the gelation point, the characteristic decay time of the fast mode, τ_{fast}, decreased, and the fraction of the collective diffusion mode, A, increased with [NCO]/[OH], which are due to introduction of cross-linking and/or increase of the rigidity of the network. Finally, the ensemble average scattering intensities, $\langle I \rangle_E$, the static inhomogeneities, $\langle I_C \rangle_E$, the time-average dynamic fluctuating component, $\langle I_F \rangle_T$ and the collective diffusion coefficient, D, showed remarkable dependence not only on C_{polyol} but also on [NCO]/[OH]. These are due to the competition between the cross-linking and the progress of micro-phase separation.

1. Introduction

Polyurethane resin is one of the most familiar materials consisting of polyisocyanate and polyol groups. Due to the good mechanical properties like adherence and durability, polyurethane resin is widely used as industrial applications in the wide ranges such as adhesives, fabrics, paints, and inks [1–3]. Polyurethane resin including isocyanurate groups, which is formed by a trimerization reaction of isocyanate groups, provides better thermal stability and rigidity than that composed of linear urethane bonding because of more functional groups and of stiffer hard segments in the former one [4–6].

As for the effect of the stoichiometric ratio, [NCO]/[OH], into the network structure of polyurethane resin, various studies have been carried out so far. Redman reported the effect of the [NCO]/[OH] ratio on molecular weight and on the rheological, thermal, and mechanical properties of two series of ester-based polyurethanes [7]. Nierzwicki and Wysocka also studied the effect of the [NCO]/[OH] ratio on the micro-phase separation of ester-based polyurethanes, which can be induced by the soft segments and hard segments, by thermo-mechanical analysis (TMA) [8]. Spathis et al. investigated the morphological changes in segmented polyurethane elastomers by Fourier transform infrared spectroscopy (FTIR) and differential scanning calorimetry (DSC) [9]. Nicolai and coworkers investigated viscoelastic relaxation of polyurethane at different stages of gel formation by focusing on glass transition dynamics and sol–gel transition dynamics [10,11].

A large number of studies on the thermal and mechanical properties and microscopic structure of polyurethane resin have been also carried out using various methods such as TMA, FTIR, DSC, small-angle angle X-ray scattering (SAXS), and wide-angle X-ray diffraction (WAXD) [4,8,9,12–14]. Dynamic light scattering (DLS) is one of the most powerful tools which can provide the information not only about the dynamics of the gelation process but also the dynamic and/or static inhomogeneities about the network structure. There have been many DLS studies that discussed concentration fluctuations of polymer solutions as a result of introduction of cross-linking [15–17]. However, to our knowledge, there have been no reports which discussed the gelation process and the microstructure focusing on the total concentration

* Corresponding author.
E-mail address: shibayama@issp.u-tokyo.ac.jp (M. Shibayama).

0032-3861/$ – see front matter © 2009 Elsevier Ltd. All rights reserved.
doi:10.1016/j.polymer.2009.03.035

and [NCO]/[OH] dependence of polyurethane gels in the presence of solvent by DLS.

In this paper, we discuss the gelation kinetics and the microstructure of polyurethane gels by focusing on the network concentration and the stoichiometric ratio of isocyanate to hydroxyl groups, [NCO]/[OH]. The purpose of this study is to clarify the following matters; first, the total concentration and [NCO]/[OH] dependence of gelation process; secondly, the effect of the total concentration and [NCO]/[OH] on the dynamic and/or static inhomogeneities of the network. We used acryl-polyol as a soft segment component and polyisocyanate as a hard segment component. The chemical structure during the reaction is shown in Fig. 1.

2. Experimental

2.1. Sample preparation

Acryl-polyol ($M_w = 4500$ and $M_n = 2600$) and polyisocyanate including isocyanurate groups were purchased from DIC, Inc. (Tokyo, Japan). Dibutyltin dilaurate (DBTDL) was purchased from Hayashi Kasei Co., Ltd. (Nagoya, Japan) and used as reaction catalyst. 2-Heptanone was purchased from Tokyo Kasei Co., Ltd. (Tokyo, Japan) and used as diluent. A series of polyurethane resin with different [NCO]/[OH]s and total concentrations were prepared with these samples without further purification.

2.2. DLS measurement

DLS studies were carried out using a DLS/SLS-5000 compact goniometer, ALV, Langen, coupled with an ALV photon correlator. A 22 mW helium–neon laser (wavelength, $\lambda = 6328$ Å) was used to deliver the incident beam. The scattering angle was 90°, or several angles in the case of q-dependent measurements, where q is the magnitude of scattering vector. As for the measurement of gelation process, the gelation reaction was performed at a high temperature in order to control and decrease the gelation time. The chemical compositions of the obtained samples and the measurement temperature are shown in Table 1. Only the samples at $C_{polyol} = 27.0$ wt% were prepared at the condition of DBTDL = 800 ppm and Temp. = 60 °C in order to reduce and control the gelation process. In addition, the gelation measurements for $C_{polyol} = 27.0$ wt% at an equal distance from T_g of bulk were also performed since the T_g varies with [NCO]/[OH]. The T_gs obtained by a viscoelastic measurement were 64.7, 67.8, 71.3, 69.9, 74.3, 73.9, 84.3, and 86.0 °C for [NCO]/[OH] = 0.8, 1.0, 1.2, 1.4, 1.6, 2.0, 3.0, and 4.0, respectively. On the other hand, in the case of the ensemble average scattering intensity measurement, gelation reaction was performed at 25 °C for 1 day in order to suppress the evaporation of the diluent. The chemical compositions of the obtained samples are shown in Table 2. The time–intensity correlation functions and the time-average scattering intensities were obtained at different 100 sample positions by rotating the sample tube (ensemble averaging). The details of the theoretical analysis were described elsewhere [18,19].

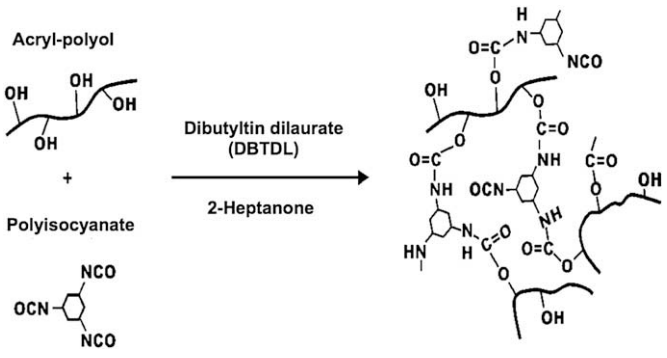

Fig. 1. Chemical structure showing the reaction on the cross-linking between acryl-polyol and polyisocyanate.

Table 1
Chemical composition of polyurethane resin used at the measurement of gelation process.

C_{polyol} (wt%)	[NCO]/[OH]	DBTDL (ppm)	Temp. (°C)
12.8	1.0, 1.2, 1.4, 2.0	2400	100
17.1	0.8, 1.0, 1.2, 1.4, 2.0, 3.0	2400	100
21.4	0.6, 0.8, 1.0, 1.2, 1.4, 2.0, 3.0	2400	100
27.0	0.6, 0.8, 1.0, 1.2, 1.4, 1.6, 2.0, 3.0, 4.0	800	60

3. Results and discussion

3.1. Sol–gel transition phase diagram

Fig. 2 shows the sol–gel transition phase diagram for polyol/polyisocyanate group systems. We determined the gelation threshold by tilting a tube method. The horizontal axis denotes the concentration of acryl-polyol and the vertical axis is the concentration of polyisocyanate. The open circles and the crosses indicate gel and sol states, respectively. The solid curve is drawn for the guide. We can conclude from Fig. 2 that the lowest polyol concentration to form a gel, C^*, exists $C_{polyol} \approx 12.8$ wt%. In addition, the following conclusion can be obtained. Not only an increase of polyisocyanate, but also an increase of acryl-polyol leads to decrease of the lower limit of the concentration for gelation. It should be noted that this type of phase behavior is theoretically predicted by the site–bond percolation theory developed by Coniglio et al. [20,21] and is experimentally observed in several systems by Shibayama et al. [22,23]. In the case of our study, the volume fraction of acryl-polyol was much higher than that of polyisocyanate. In other words, an increase of acryl-polyol leads to site-percolation while an increase of polyisocyanate induces bond-percolation like chemical cross-linker.

3.2. Gelation process

Fig. 3 shows a typical example of the time evolution of the scattering intensity, $\langle I \rangle_T$, and the initial amplitude of the time–intensity correlation function (ICF), σ_I^2 ($=g^{(2)}(0) - 1$). The sample of $C_{polyol} = 27.0\%$ and [NCO]/[OH] = 1.0 was shown here. During the gelation process, $\langle I \rangle_T$ gradually increased. Then $\langle I \rangle_T$ started to drastically increase and σ_I^2 started to decrease at about $t = 90$ min. The decrease of σ_I^2 means an increase of static inhomogeneities due to the sol–gel transition. It should be noted that $\langle I \rangle_T$ did not increase instantaneously while the conventional gelation process occurred accompanying instantaneous increase of $\langle I \rangle_T$ as has been studied by many workers [16,24]. This is because the gelation proceeded from

Table 2
Chemical composition of polyurethane resin used at the measurement of 100 sample positions.

C_{polyol} (wt%)	[NCO]/[OH]	DBTDL (ppm)
12.8	1.0, 1.2, 1.6, 2.0, 2.5, 3, 4, 5	2400
17.1	0.8, 1.0, 1.2, 1.4, 1.6, 2.0, 2.5, 4.0	2400
21.4	0.6, 0.8, 1.0, 1.2, 1.4, 1.6, 2.0, 2.5	2400
27.0	0.4, 0.6, 0.8, 1.0, 1.2, 1.4, 1.6, 2.0, 2.5, 3.0, 4.0	800
32.1	0.4, 0.6, 0.8, 1.0, 1.2, 1.4, 1.6, 2.0, 2.5, 3.0, 4.0	800

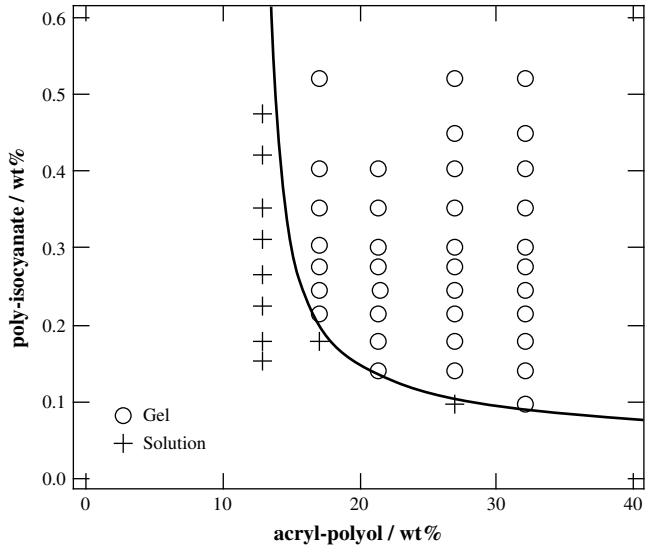

Fig. 2. The sol–gel transition phase diagram for polyol/polyisocyanate group systems. (a) The sol–gel transition behavior of polyol as a function of [NCO]/[OH]. (b) The sol–gel transition behavior according to the site–bond percolation theory.

the oligomer state of polyol by skipping monomer to oligomer process.

Fig. 4 shows an example of time evolution of the time–intensity correlation functions, $g^{(2)}(\tau)-1$, for the sample of $C_{\text{polyol}}=27.0\%$ and [NCO]/[OH] = 1.0. The solid line at 91.6 min indicates the result of curve fitting as discussed below. The dynamics of gelation process can be divided into the following three stages. In the first stage, the translational diffusion of the oligomer of polyol was observed. The second stage corresponds to the gelation point, where $g^{(2)}(\tau)-1$ showed a power-law behavior. In the third stage, i.e., in the post-gelation stage, σ_I^2 decreased as discussed above. As for the power-law behavior at the gelation point, ICFs can be described by the following functions [25,26]:

$$g^2(\tau)-1\approx\sigma_I^2\left\{A\exp(-\tau/\tau_{\text{fast}})+(1-A)\left[1+\left(\tau/\tau^*\right)\right]^{(n-1)/2}\right\}^2 \quad (1)$$

where A is the fraction of the collective diffusion mode, τ_{fast} is the characteristic decay time of the fast mode, τ^* is the characteristic

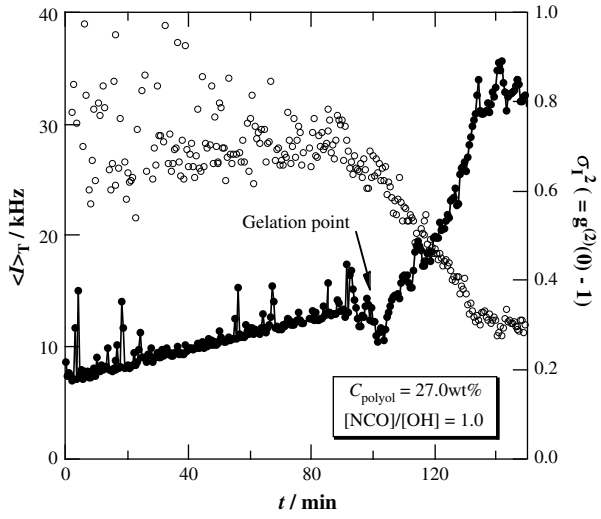

Fig. 3. A typical example of the time evolution of the scattering intensities, $\langle I\rangle_T$, and the initial amplitude of the time–intensity correlation function (ICF), σ_I^2 ($=g^{(2)}(0)-1$) The sample of $C_{\text{polyol}}=27.0\%$ and [NCO]/[OH] = 1.0 is shown here.

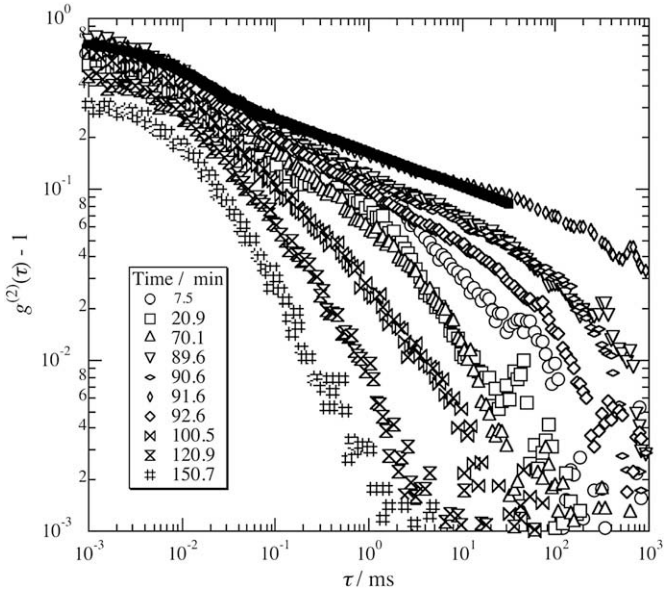

Fig. 4. A typical example of the time evolution of the time–intensity correlation functions, $g^{(2)}(\tau)-1$. The sample of $C_{\text{polyol}}=27.0\%$ and [NCO]/[OH] = 1.0 is shown here.

time where the power-law behavior appears, and n is the fractal dimension of the scattered photons.

Fig. 5 shows a typical example of q dependence of the decay rate, Γ, for the fast mode shown in Fig. 4, for the sample of $C_{\text{polyol}}=27.0\%$ and [NCO]/[OH] = 1.0. Γ was obtained from the decay rate distribution function and CONTIN program [27], the detail was shown elsewhere [28]. As shown here, the relaxation mode clearly shows q^2 dependence of Γ, confirming that the relaxation mode is diffusive. Therefore, we can conclude that the molecular motion of this system does not correspond to Rouse or Zimm mode, but to a diffusion mode.

Fig. 6(a) shows [NCO]/[OH] dependence of the gelation time, t_{gel}, for various C_{polyol}s. Note that the reaction temperature for the sample of $C_{\text{polyol}}=27.0$ wt% (60 °C) was lower than the

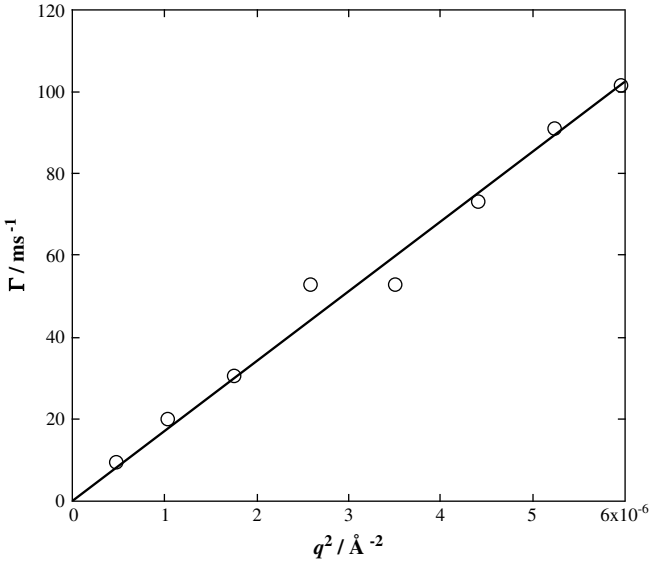

Fig. 5. A typical example of q dependence of the decay rate, Γ, for the fast mode shown in Fig. 4. The sample of $C_{\text{polyol}}=27.0\%$ and [NCO]/[OH] = 1.0 is shown here.

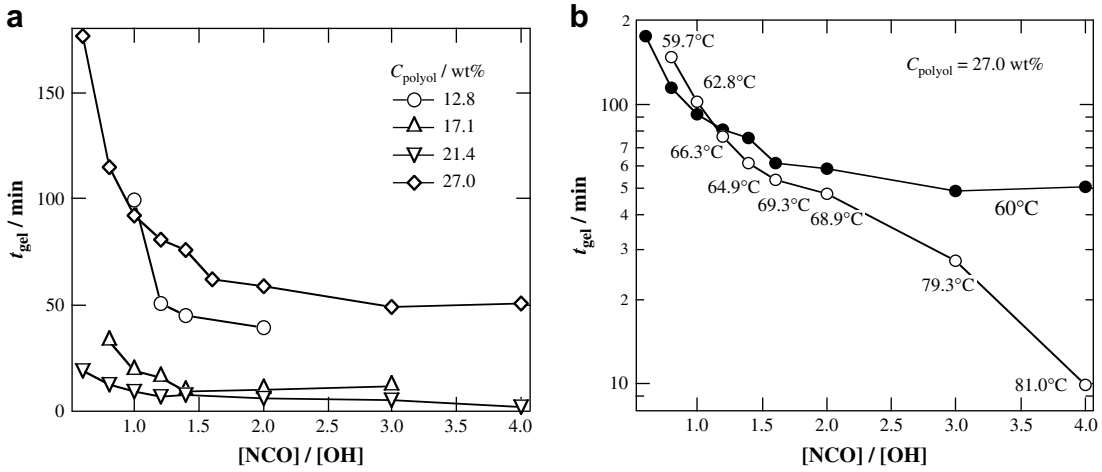

Fig. 6. [NCO]/[OH] and C_{polyol} dependence of the gelation time, t_{gel}. Closed symbols and open symbols indicate the measurements where the observation temperature was constant and the distance from T_g was constant, respectively.

others (100 °C) and the concentration of the catalyst (DBTDL) was lower, leading to a larger t_{gel}. For the samples prepared at $C_{polyol} \leq 21.4$ wt%, t_{gel}s decreased with C_{polyol}, while its [NCO]/[OH] dependence was insignificant compared with those at $C_{polyol} = 27.0$ wt%. In the case of $C_{polyol} = 27.0$ wt%, on the other hand, t_{gel} is a strong decreasing function of [NCO]/[OH]. The decrease in t_{gel} with increasing [NCO]/[OH] means that the gelation reaction is accelerated by increasing cross-linker concentration. The little [NCO]/[OH] dependence for the samples of $C_{polyol} \leq 21.4$ wt% indicates the catalyst concentration was too large and the reaction temperature was too high for gelation.

Fig. 6(b) shows the comparison of the t_{gel}s between the measurement where observing temperature is constant (closed symbols) and where the distance from T_g is constant (open symbols). In any case, t_{gel} decreased with [NCO]/[OH]. At low [NCO]/[OH] region, the difference of t_{gel}s at a given [NCO]/[OH] is negligible since the temperature is close to each other while the obvious distinction appeared with the increase of [NCO]/[OH].

Fig. 7(a)–(c) shows τ^*, τ_{fast}, A, and n for the case of $C_{polyol} = 27.0\%$ at a gelation point obtained with Eq. (1), respectively. Closed symbols and open symbols indicate the measurement where observing temperature is constant and where the distance from T_g is constant, respectively. It is obvious that τ_{fast} and A showed the characteristic behavior depending on [NCO]/[OH]. At the gelation point, an infinite network was formed, leading to the decrease of τ_{fast}, in other words, the decrease of the correlation length. However, it should be noted that the cross-linking proceeds rather gradually in this system as shown in Fig. 3. Therefore, the [NCO]/[OH] dependence of τ_{fast} and A may indicate not only the effect of cross-linking but also the rise of the elasticity by the rigidity of isocyanurate groups, which will be discussed below. On the other hand, n was constant with respect to [NCO]/[OH]. Since n is known to be related to the branch degree of the cluster at the gelation, we can conclude that the increase of [NCO]/[OH] does not influence the degree of branching of this system. As for the difference of the measurement temperature, it is obvious that the trend of [NCO]/[OH] dependence of each parameter is the same between the two. This is due to the fact that the gelation measurement was performed for the samples including a large amount of solvent. Therefore, the measuring temperature, or the dynamics of the glass transition, can be negligible compared with the sol–gel transition dynamics. The observation of gelation dynamics for bulk systems will be disclosed in the near future.

3.3. Microscopic inhomogeneities after gelation

3.3.1. $\langle I \rangle_T$ at 100 different sample positions for the gel and sol state

Fig. 8 shows the time-average scattering intensities, $\langle I \rangle_T$, at 100 different sample positions for typical examples of (a) gel state and (b) sol state. For (a) and (b), $C_{polyol} = 27.0\%$ and [NCO]/[OH] = 1.0,

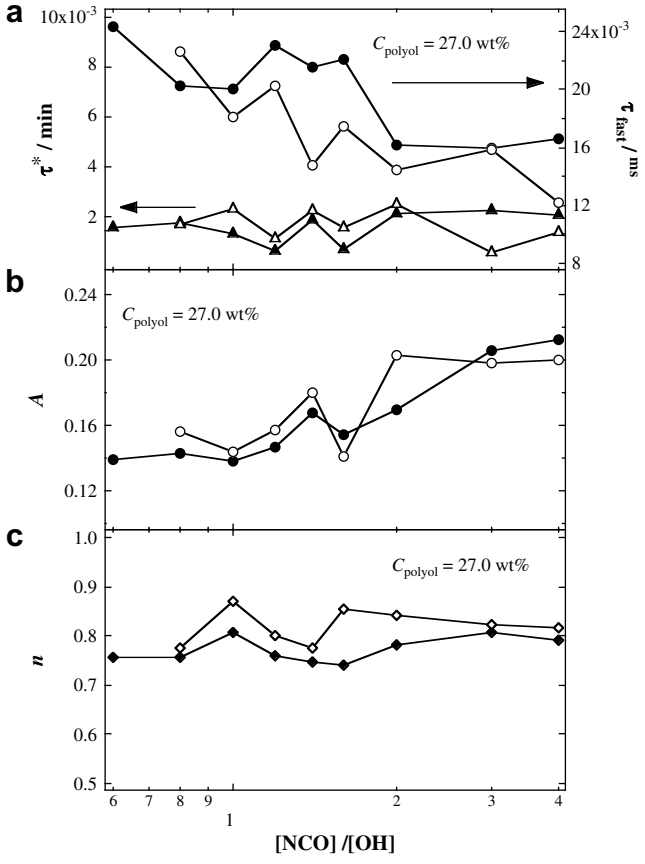

Fig. 7. A typical example of (a) τ^* and τ_{fast}, (b) A, and (c) n for $C_{polyol} = 27.0\%$ at a gelation point obtained with Eq. (1). Closed symbols and open symbols indicate the measurements where the observation temperature was constant and the distance from T_g was constant, respectively.

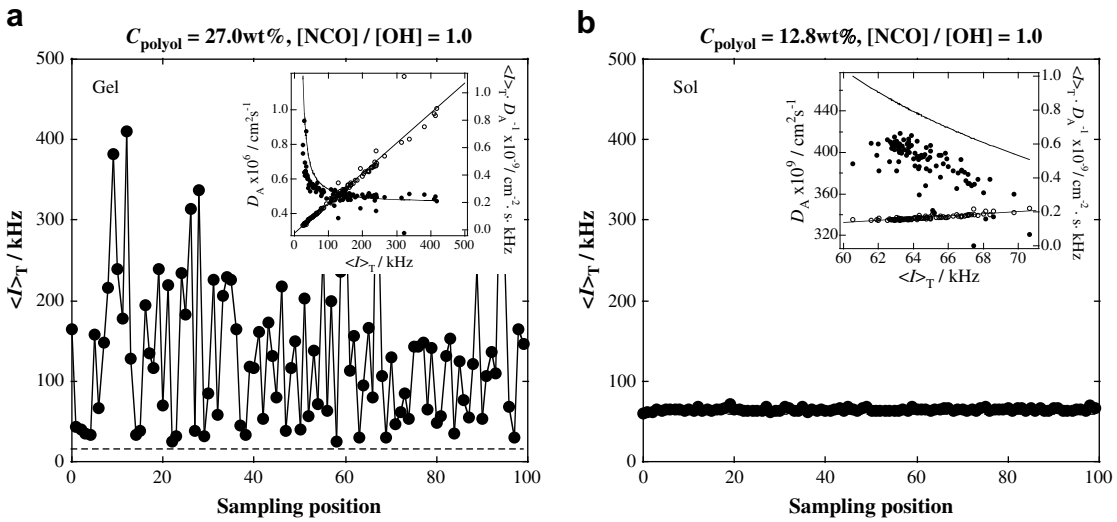

Fig. 8. The time-average scattering intensities, $\langle I\rangle_T$, at 100 different sample positions for typical examples of (a) gel state and (b) sol state. For (a) and (b), $C_{polyol} = 27.0\%$ and [NCO]/[OH] = 1.0 and $C_{polyol} = 12.8\%$ and [NCO]/[OH] = 1.0, respectively.

and $C_{polyol} = 12.8\%$ and [NCO]/[OH] = 1.0, respectively. The broken line indicates the dynamic fluctuating component, $\langle I_F\rangle_T$. The insets show the apparent diffusion coefficient, D_A, as a function of $\langle I\rangle_T$ and a replot for the derivation of $\langle I_F\rangle_T$ and the collective diffusion coefficient, D. According to Joosten et al., D can be evaluated by plotting D_A as a function of $\langle I\rangle_T$ by using the following equation [18]:

$$D_A = \frac{D}{2 - \langle I_F\rangle_T/\langle I\rangle_T} \tag{2}$$

We can rewrite Eq. (2) and obtain the following relationship [15,29]:

$$\frac{\langle I\rangle_T}{D_A} = \frac{2}{D}\langle I\rangle_T - \frac{\langle I_F\rangle_T}{D} \tag{3}$$

Once $\langle I_F\rangle_T$ is obtained, the static inhomogeneities, $\langle I_C\rangle_E$, are easily obtained by

$$\langle I_C\rangle_E \equiv \langle I\rangle_E - \langle I_F\rangle_T \tag{4}$$

where $\langle I\rangle_E$ is the ensemble average scattering intensities of $\langle I\rangle_T$. The solid lines in the insets indicate the fitting curves with Eq. (2) or (3).

By comparing Fig. 8(a) and (b), it is obvious that $\langle I\rangle_T$s in gel state strongly depend on the sample position, i.e., the large static inhomogeneities exist. On the other hand, $\langle I\rangle_T$s at sol state do not depend on the sample position and the contribution of $\langle I_C\rangle_E$ to $\langle I\rangle_E$ is ignorable. These are typical trends of sol–gel systems. As for the behavior of D_A and $\langle I\rangle_T D_A^{-1}$ (in the inset), it seems that $\langle I\rangle_T D_A^{-1}$s are well fitted by Eq. (3) for both gel and sol states. However, D_A for the sol state extremely deviates from the fitting curves while that for the gel state well satisfies Eq. (2). This deviation is due to the fact that $\langle I\rangle_T$s do not show any sample position dependence, resulting in the decrease of the statistical precision and the accuracy of the determination of D and $\langle I_F\rangle_T$.

3.3.2. [NCO]/[OH] and C_{polyol} dependence of $\langle I\rangle_E$, $\langle I_C\rangle_E$, and $\langle I_F\rangle_T$

Fig. 9 shows [NCO]/[OH] and C_{polyol} dependence of (a) $\langle I\rangle_E$, (b) $\langle I_C\rangle_E$, and (c) $\langle I_F\rangle_T$. The solid lines and broken line denote gel states and a sol state, respectively.

First of all, it should be noted that $\langle I\rangle_E$ and $\langle I_C\rangle_E$ of gel states have a peak in their [NCO]/[OH] dependence and these peaks shift toward lower [NCO]/[OH] by increasing C_{polyol} while $\langle I_F\rangle_T$ shows no [NCO]/[OH] dependence. The presence of a maximum with respect to [NCO]/[OH] was reported by Nierzwicki and Wysocka about glass transition temperature, T_g, and the tensile strength properties [8]. They showed that the rise of [NCO]/[OH] leads to not only an increase of cross-linking density but also a progress of micro-phase

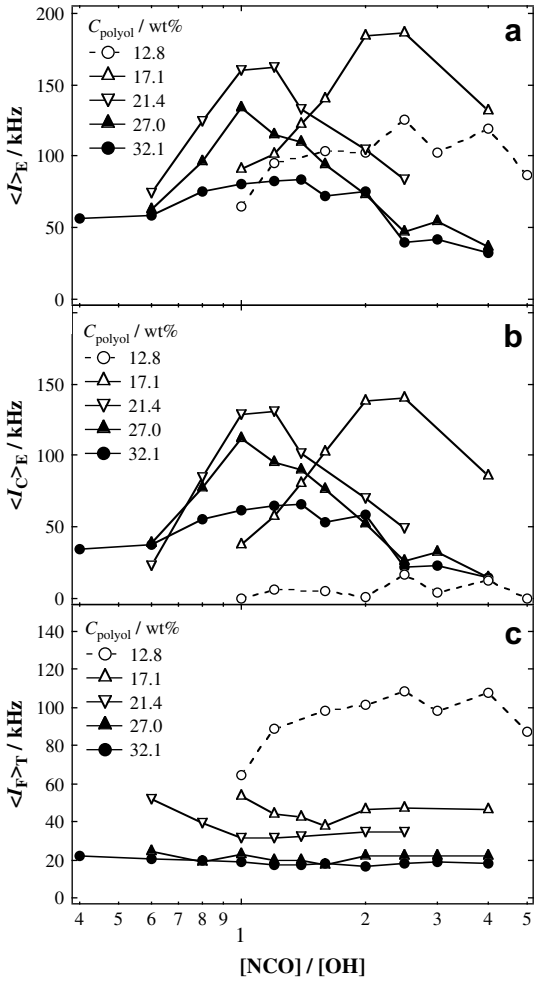

Fig. 9. [NCO]/[OH] and C_{polyol} dependence of (a) $\langle I\rangle_E$, (b) $\langle I_C\rangle_E$, and (c) $\langle I_F\rangle_T$. The solid lines and dashed line mean that the system is gel states and sol states, respectively.

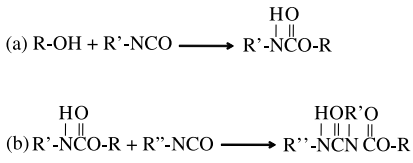

Fig. 10. Chemical schemes of (a) urethane bond structure and (b) allophanate structure.

separation accompanying formation of allophanate groups caused by the excess of NCO groups (see Fig. 10). If the network structure was determined by the former, the maximum should be at [NCO]/[OH] = 1. However, the latter factor immobilizes the hard segments (NCO groups) causing T_g upward. As a result, the optimum of T_g and the tensile strength properties can shift above [NCO]/[OH] = 1.

In the case of our results, on the other hand, the maximum of $\langle I\rangle_E$ and $\langle I_C\rangle_E$ was around [NCO]/[OH] = 1 at $C_{polyol} > 17.1$ wt% while that shifted toward higher [NCO]/[OH] at $C_{polyol} = 17.1$ wt%. That is to say, at $C_{polyol} > 17.1$ wt%, the cross-linking was mainly formed and the cross-linking density became maximum at around [NCO]/[OH] = 1, leading to the increase of the concentration fluctuation by the introduction of the cross-linking. However, at $C_{polyol} = 17.1$ wt%, allophanate structure may be also formed due to the high mobility and reactivity of the components at a dilute regime, resulting in the progress of micro-phase separation composed of soft and hard segments. To our knowledge, this is the first observation of such a shift of the maximum by DLS.

Next, let us discuss the C_{polyol} dependence of $\langle I\rangle_E$, $\langle I_C\rangle_E$, and $\langle I_F\rangle_T$. As shown in Fig. 9(a) and (b), $\langle I\rangle_E$ and $\langle I_C\rangle_E$ decreased by the increase of C_{polyol} except for the results of $C_{polyol} = 12.8$ wt%, which are at sol states. The decreases of $\langle I\rangle_E$ and $\langle I_C\rangle_E$ indicate that the suppression of the concentration fluctuation increased with the total network concentration over the chain overlap concentration. On the other hand, the lower $\langle I\rangle_E$ and $\langle I_C\rangle_E$ of $C_{polyol} = 12.8$ wt% than the other samples at gel states are due to the fact that $\langle I_C\rangle_E$ at a sol state is composed only of $\langle I_F\rangle_T$. Therefore, the lowering shift of $\langle I_F\rangle_T$ with C_{polyol} corresponds to the transition from a sol to a gel state.

3.3.3. [NCO]/[OH] and C_{polyol} dependence of D

Fig. 11 shows [NCO]/[OH] and C_{polyol} dependence of D. The solid lines and broken line denote gel states and a sol state, respectively.

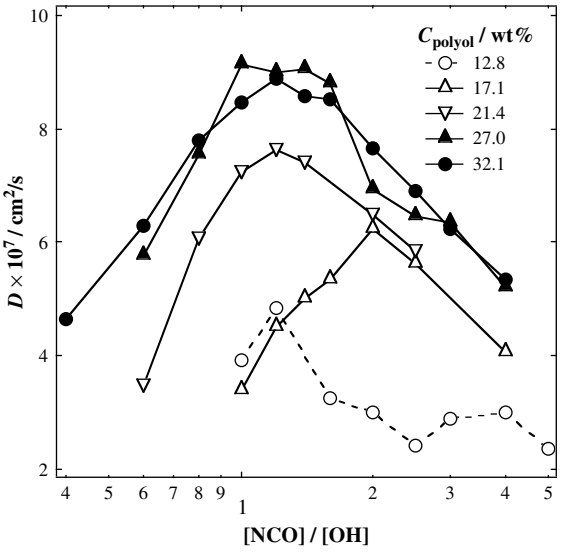

Fig. 11. [NCO]/[OH] and C_{polyol} dependence of D. The solid lines and dashed line mean that the system is gel states and sol states, respectively.

First, D increased with C_{polyol} whether the sample was gel or sol states. It is known that D is related to the correlation length, ξ, with the following equation [15,30]:

$$D \approx \frac{k_B T}{6\pi\eta\xi} \tag{5}$$

where k_BT and η denote the Boltzmann energy and the solvent viscosity, respectively. Therefore, the increase of D corresponds to the decrease of ξ due to the suppression of the concentration fluctuations. Secondly, the clear convex behavior and the interesting shift of the maximum with respect to [NCO]/[OH] were also observed here. This experimental result supports the above discussions. The maximum of ξ at the stoichiometric ratio, i.e., [NCO]/[OH] ≈ 1, indicates that the finest network is formed at this ratio. The shift of the peak position for the case of $C_{polyol} = 17.1$ wt% is probably due to the additional effect by formation of allophanate structure which becomes dominant at lower polyol concentrations. Further investigations regarding these mechanical properties are in progress.

4. Conclusions

The [NCO]/[OH] and C_{polyol} dependence of the gelation process and the microstructure after the gelation of polyurethane resin were investigated by DLS. The following conclusions were obtained. First, the sol–gel transition was explained by the so-called site–bond percolation theory. Here, polyol groups act as site-occupants and isocyanate groups, which is composed of isocyanurate structure, act as chemical cross-linkers. Second, the scattering inhomogeneities were rather gradually increased around the gelation point, which are the characteristics of the gelation process from oligomer units. In addition, the τ_{fast} and A of the structural parameters at the gelation point were strongly dependent on [NCO]/[OH], which may be due to the introduction of the cross-linking and the increase of network rigidity. Finally, $\langle I\rangle_E$, $\langle I_C\rangle_E$, $\langle I_F\rangle_T$ and D showed characteristic dependence on C_{polyol} and [NCO]/[OH]. With the increase of C_{polyol}, $\langle I\rangle_E$ and $\langle I_C\rangle_E$ at the gel states decreased due to the suppression of the concentration fluctuation. $\langle I_F\rangle_T$ also decreased with C_{polyol} due to the decrease of the solution components. On the other hand, D increased with C_{polyol} indicating the decrease of the correlation length of the networks. As for the [NCO]/[OH] dependence, at $C_{polyol} > 17.1$ wt%, $\langle I\rangle_E$, $\langle I_C\rangle_E$, and D showed a maximum at around [NCO]/[OH] = 1 because the cross-linking density mainly influences the microscopic network structure. However, at $C_{polyol} = 17.1$ wt%, the maximum of [NCO]/[OH] shifted upward because not only the cross-linking density but also the progress of micro-phase separation resulting from the excess of hard segment dominated the network structure.

Acknowledgement

This work was supported by the Ministry of Education, Science, Sports and Culture, Japan (Grant-in-Aid for Scientific Research on Priority Areas, 2006–2010, No. 18068004).

References

[1] Ratner BD. Comprehensive polymer science. New York: Pergamon Press; 1988.
[2] Plank H, Egbers G, Syre I. Polyurethanes in biomedical engineering. Amsterdam: Elsevier; 1984.
[3] Lelar MD, Cooper SL. Polyurethanes in medicine. New York: CRC Press; 1986.
[4] Semsarzadeh MA, Navarchian AH. J Appl Polym Sci 2003;90:963–72.
[5] Dick C, Dominguez RB. Polymer 2001;42:913–23.
[6] Modesti M, Lorenzetti A. Eur Polym J 2001;37:949–54.
[7] Redman RP. Developments in polyurethanes. London: Applied Science Publishers; 1978.

[8] Nierzwicki W, Wysocka E. J Appl Polym Sci 1980;25:739–46.
[9] Spathis G, Niaounakis M, Contov E, Apekis L, Pissis P, Christodoulides C. J Appl Polym Sci 1994;54:831–42.
[10] Nicolai T, Randrianantoandro H, Prochazka F, Durand D. Macromolecules 1997;30:5897–904.
[11] Randrianantoandro H, Nicolai T, Durand D, Prochazka F. Macromolecules 1997;30:5893–6.
[12] Zhang Y, Shang S, Zhang X, Wang D, Hourston DJ. J Appl Polym Sci 1996;59:1167–71.
[13] Huang J, Zhang L. Polymer 2002;43:2287–94.
[14] Ikkai F, Shibayama M, Kashihara H, Nomura S. Polymer 1997;38:769–74.
[15] Shibayama M, Norisuye T, Nomura S. Macromolecules 1996;29:8746–50.
[16] Norisuye T, Shibayama M, Nomura S. Polymer 1998;39(13):2769–75.
[17] Suzuki T, Ikkai F, Shibayama M. Macromolecules 2007;40:2509–14.
[18] Joosten JGH, McCarthy JL, Pusey PN. Macromolecules 1991;24(25):6690–9.
[19] Pusey PN, van Megen W. Physica A 1989;157:705–41.
[20] Coniglio A, Stanley HE, Klein W. Phys Rev Lett 1979;42:518–22.
[21] Coniglio A, Stanley HE, Klein W. Phys Rev B 1982;25:6805–21.
[22] Shibayama M, Norisuye T. Bull Chem Soc Jpn 2002;75:641–59.
[23] Takeda M, Norisuye T, Shibayama M. Macromolecules 2000;33:2909–15.
[24] Kobayashi S. Rev Sci Instrum 1985;56(1):160–2.
[25] Martin JE, Adorf D, Wilcoxon JP. Phys Rev Lett 1988;61:2620–3.
[26] Martin JE, Wilcoxon J, Odinek J. Phys Rev A 1991;43:858–71.
[27] Provencher SW. Comput Phys Commun 1982;27:213–27.
[28] Shibayama M, Isaka Y, Shiwa Y. Macromolecules 1999;32:7086–92.
[29] Shibayama M, Fujikawa Y, Nomura S. Macromolecules 1996;29(20):6535–40.
[30] de Gennes PG. Scaling concepts in polymer physics. Ithaca: Cornell University; 1979.